Electronic Supplementary Information

Polyoxometalate Complexes for Oxidative Kinetic Resolution of Secondary Alcohols: Unique Effects of Chiral Environment, Immobilization and Aggregation

Lei Shi, Yizhan Wang, Bao Li and Lixin Wu*

State Key Laboratory of Supramolecular Structure and Materials, College of Chemistry, Jilin University,

Changchun 130012, China.

To whom correspondence should be addressed. E-mail: wulx@jlu.edu.cn.

Characterization for Chiral Surfactants:

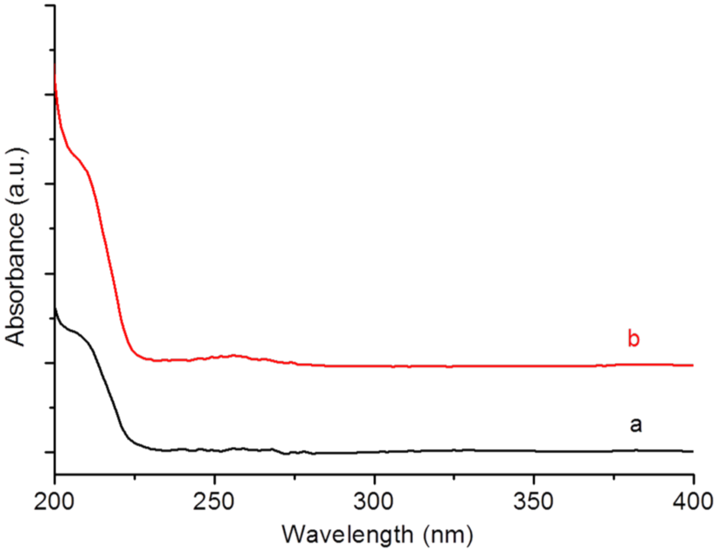

Figure S1. UV-Vis spectra of (a) R-DOHPA·Br and (b) S-DOHPA·Br in CH_3CN.

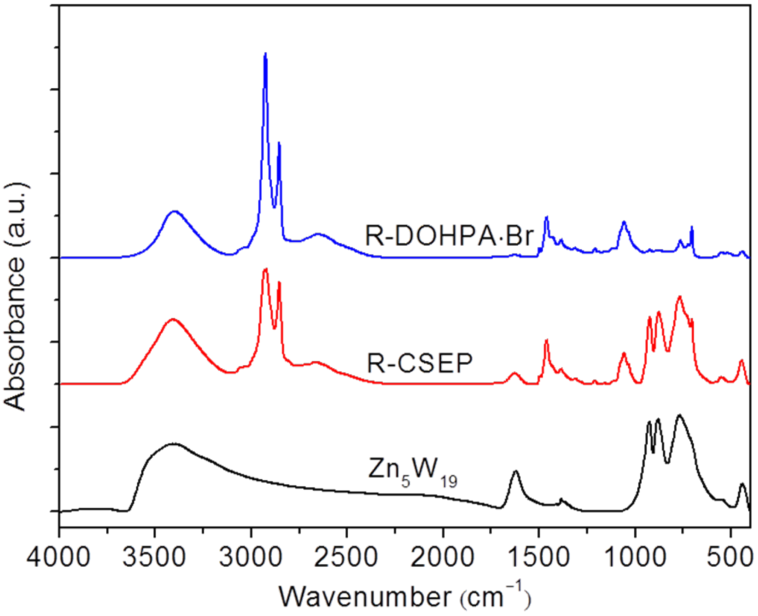

Figure S2. FT-IR spectra of R-DOHPA·Br, R-CSEP and Zn_5W_{19} in KBr pellets.

Table S1. The assignment of the characteristic vibrational bands of R-DOHPA·Br, R-CSEP and Zn_5W_{19}.

R-DOHPA·Br (cm^{-1})	R-CSEP (cm^{-1})	Zn_5W_{19} (cm^{-1})	Assignment[a]
3408	3408	3398	ν_{as} (O–H)
2926	2926	-	ν_{as} (CH_2)
2854	2854	-	ν_s (CH_2)
-	1630	1630	δ (O–H)
1460	1460	-	δ (CH_2)
-	1385	1385	δ (CH_2)
1058	1058	-	ν_s (C–N)
-	924	925	ν_{as} (W=O_d)
-	878	879	ν_{as} (W–O_b–W)
-	766	769	ν_{as} (W–O_c–W)

[a] ν_{as}: antisymmetrical stretching; ν_s: symmetrical stretching; δ: scissoring stretching.

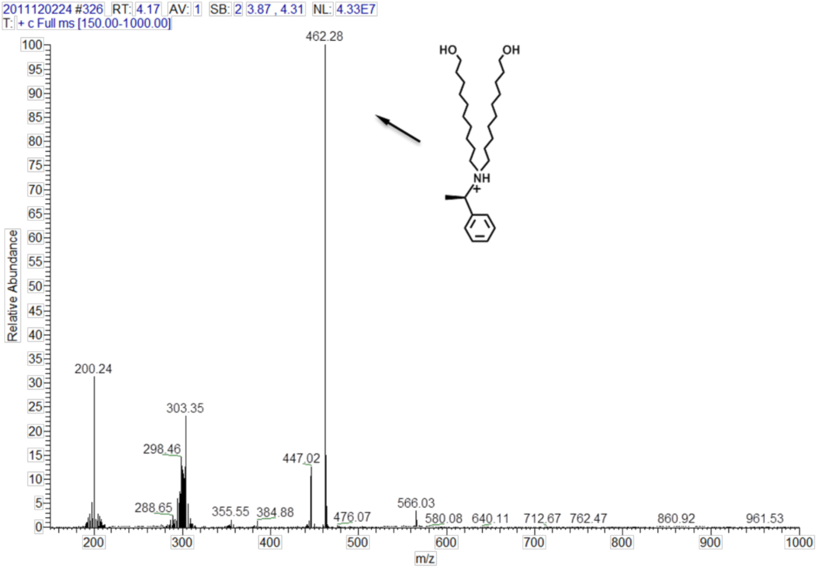

Figure S3. ESI-MS spectra of R-DOHPA·Br, in which the m/z at 462.3 is in agreement with calculated molecular weight (462.7) of [R-DOHPA]$^+$.

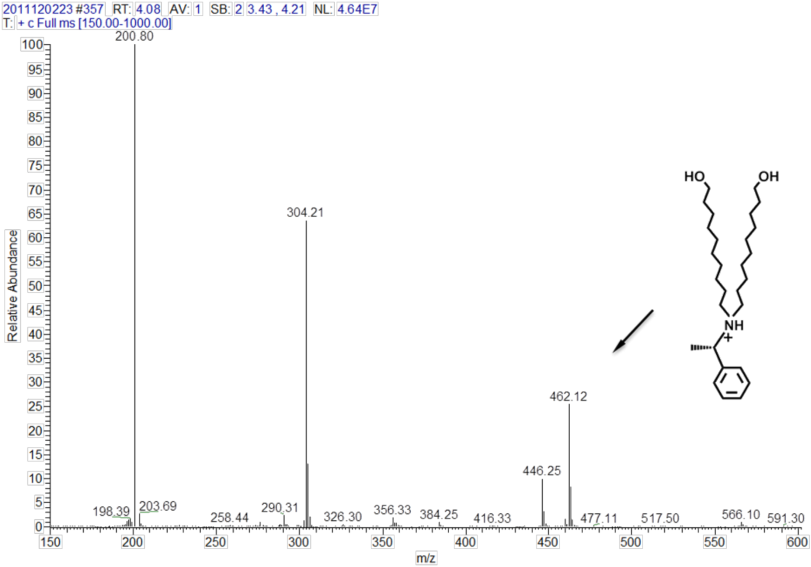

Figure S4. ESI-MS spectra of S-DOHPA·Br, in which the m/z at 462.1 is in agreement with calculated molecular weight (462.7) of [S-DOHPA]$^+$.

Characterization for CSEPs:

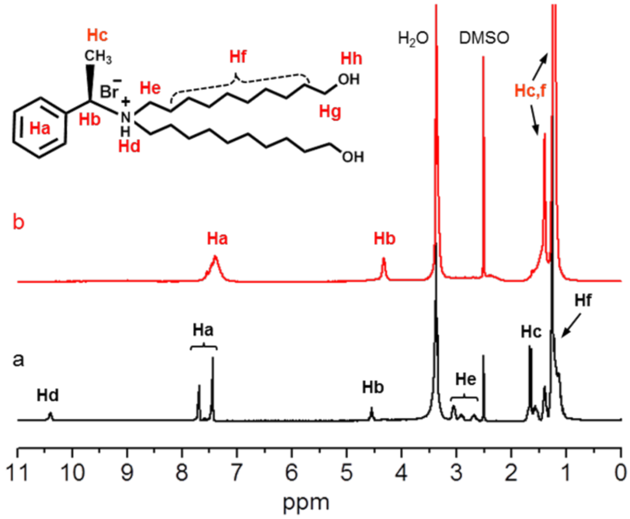

Figure S5. ^{1}H NMR spectra of (a) R-DOHPA·Br and (b) R-CSEP in DMSO-d_6, in which H_h is not detectable and H_g overlaps with the H_2O peak at ca. 3.34 ppm.

Table S2. The chemical shifts of protons on the chiral carbon (H_b) of R-DOHPA·Br and R-CSEP in CD_3CN and DMSO-d_6.

Sample	CD_3CN	DMSO-d_6
R-DOHPA·Br	4.37	4.55
R-CSEP	3.97	4.33
Chemical shift	0.40	0.22

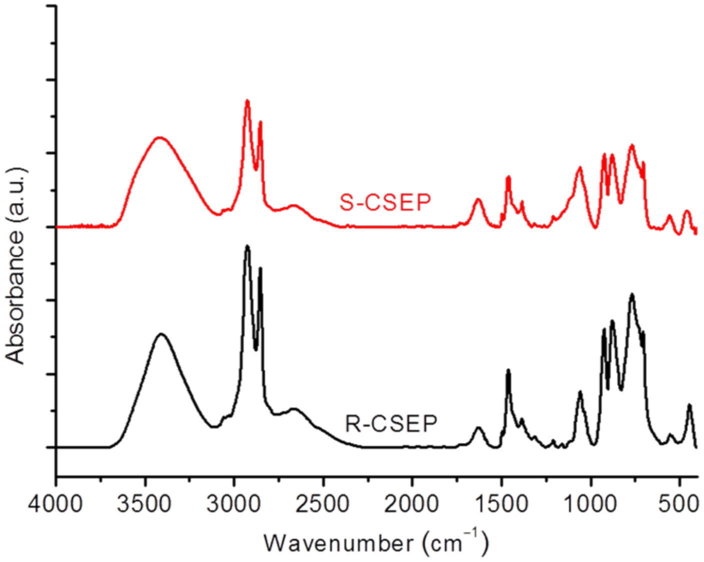

Figure S6. FT-IR spectra of R-CSEP and S-CSEP in KBr pellets.

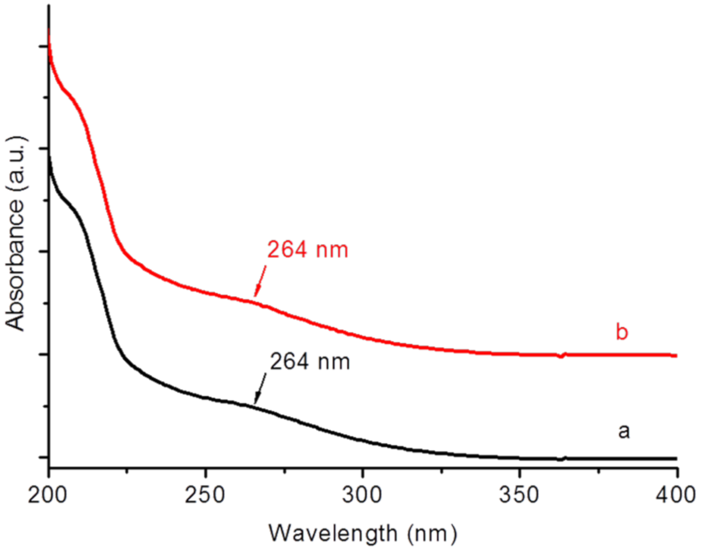

Figure S7. UV-Vis spectra of (a) R-CSEP and (b) S-CSEP in CH_3CN. The broad shoulders centered at about 264 nm can be assigned to the O → W LMCT bands in POM clusters.

Table S3. EA results of R-CSEP and S-CSEP.

$(C_{30}H_{56}NO_2)_{12}WZn_3(ZnW_9O_{34})_2$		C [%]	H [%]	N [%]
R-CSEP	Found	41.69	6.30	1.65
	Calc.	41.33	6.47	1.61
S-CSEP	Found	40.91	6.43	1.72
	Calc.	41.33	6.47	1.61

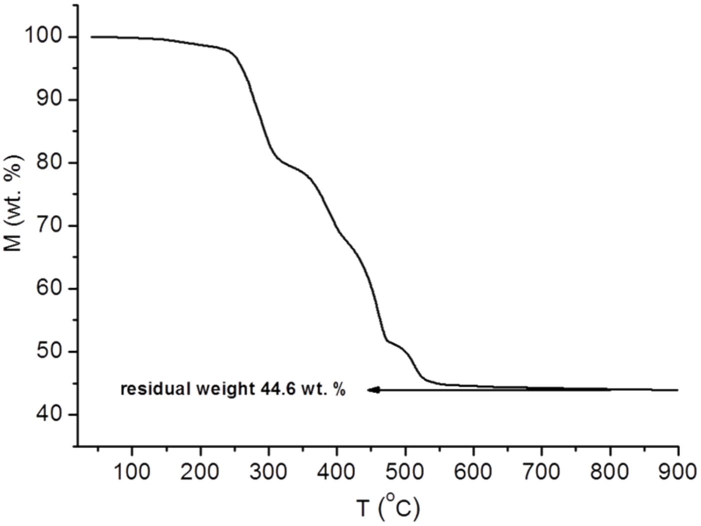

Figure S8. TGA curve of R-CSEP. The measured residue is 44.6%, in agreement with the calculated value 45.6% from the given R-CSEP formula by assuming that the organic component has decomposed completely and all the inorganic residuals are WO_3 and ZnO at 800 °C.

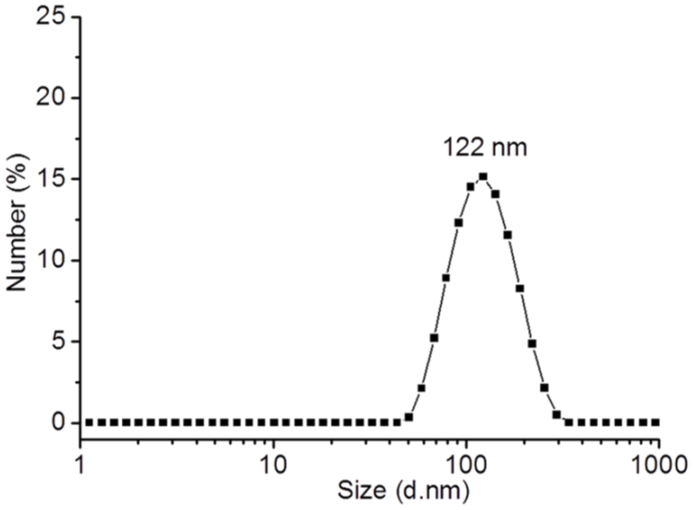

Figure S9. DLS plot of R-CSEP in ethanol (PDI = 0.232) at 25 °C. The concentration is 2.0×10^{-5} mol L^{-1}.

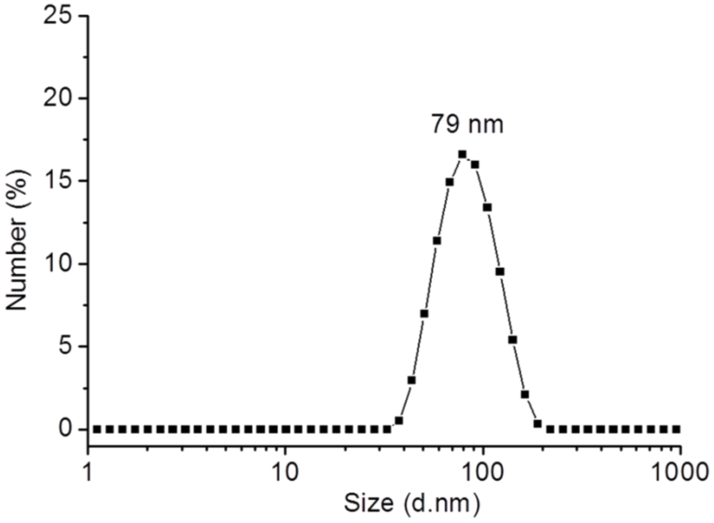

Figure S10. DLS plot of R-CSEP in acetonitrile (PDI = 0.109) at 25 °C. The concentration is 2.0×10^{-5} mol L^{-1}.

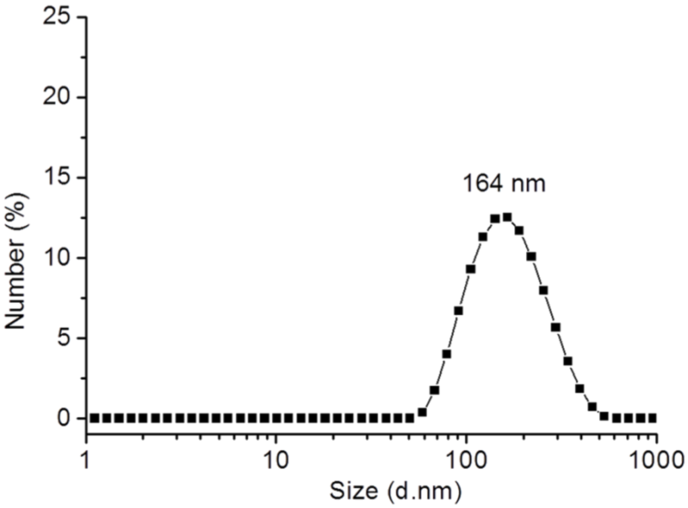

Figure S11. DLS plot of R-CSEP in acetone (PDI = 0.197) at 25 °C. The concentration is 1.5 × 10^{-5} mol L^{-1}.

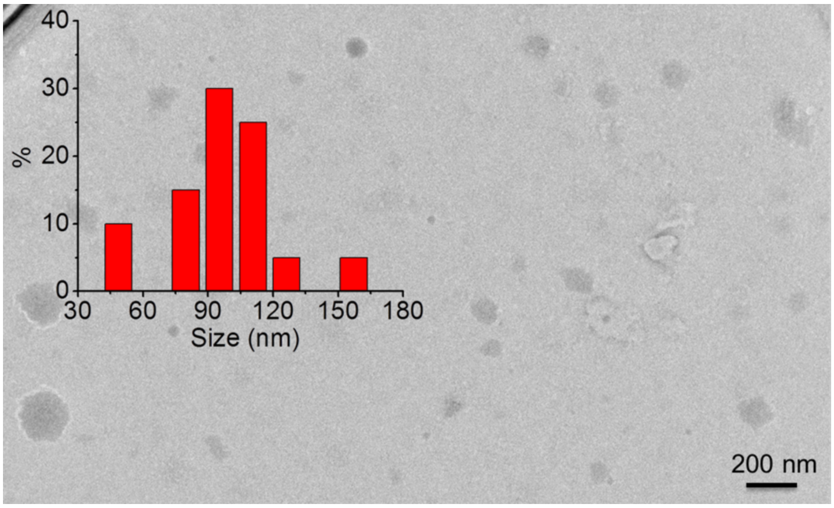

Figure S12. Representative HR-TEM image of R-CSEP complexes prepared in ethanol. The inset indicates the aggregation size distribution, where spheroids are found to be predominant and their average size is located at ca. 110 nm.

Characterization for CSHCs:

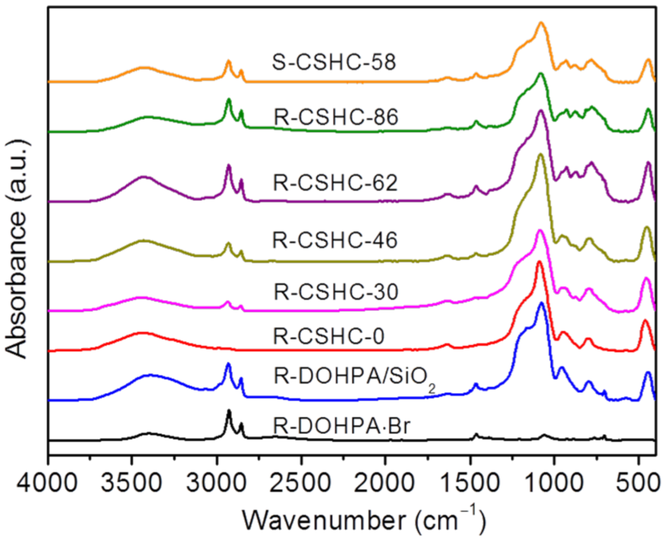

Figure S13. FR-IR spectra of R-DOHPA·Br, R-DOHPA/SiO2, R-CSHC-0, R-CSHC-30, R-CSHC-46, R-CSHC-62, R-CSHC-86 and S-CSHC-58 in KBr pellets.

Table S4. The EA results of R-DOHPA/SiO$_2$, R-CSHC-30, R-CSHC-46, R-CSHC-62, R-CSHC-86 and S-CSHC-58.

Sample	Calc. [wt. %]	N [%]	C [%]	H [%]	Found [wt. %]
R-DOHPA/SiO$_2$	45	1.38	34.43	6.03	45
R-CSHC-30	30	0.62	12.52	2.35	30
R-CHSC-46	45	0.78	19.31	3.32	46
R-CSHC-62	60	1.07	26.09	4.16	62
R-CSHC-86	80	1.45	35.88	5.62	86
S-CSHC-58	60	0.98	24.14	3.97	58

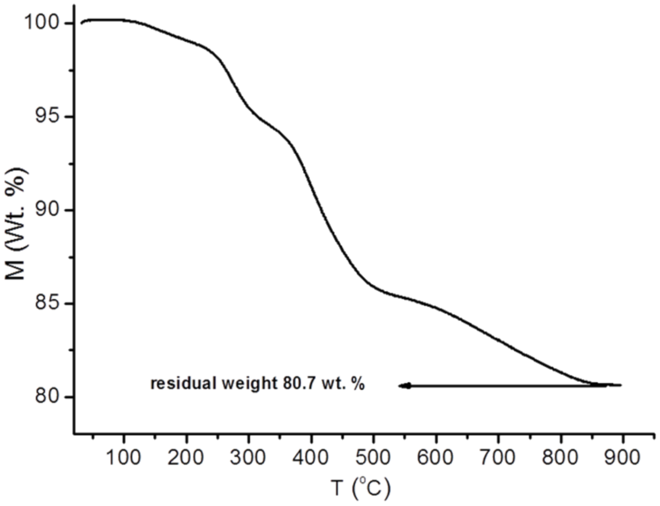

Figure S14. TGA curve of R-CSHC-30 with the residue of 80.7% at 900 °C, in agreement with the calculated value of 81.6% according to the used complex concentration, which is carried out in air with heating rate of 10 °C min^{-1}.

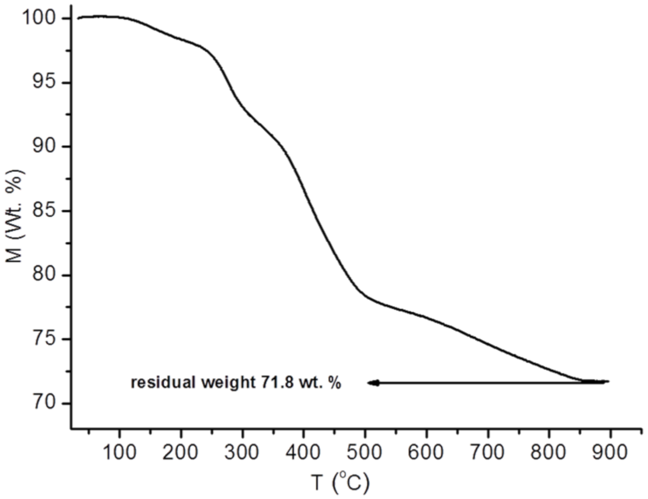

Figure S15. TGA curve of R-CSHC-46 with the residue of 71.8% at 900 °C, in agreement with the calculated value of 72.6% according to the used complex concentration, which is carried out in air with heating rate of 10 °C min^{-1}.

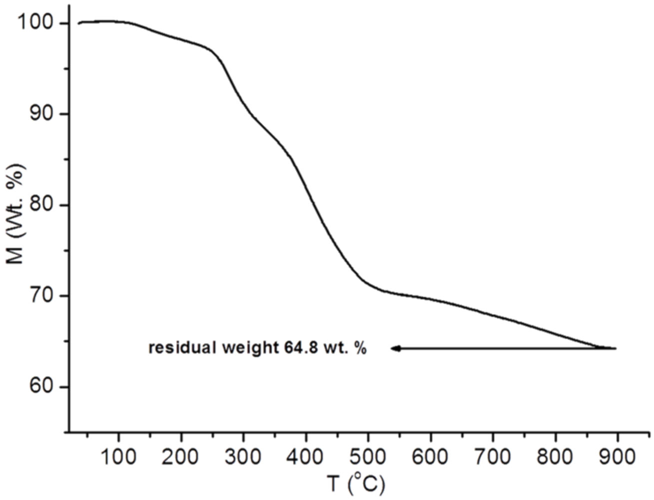

Figure S16. TGA curve of R-CSHC-62 with the residue of 64.8% at 900 °C, in agreement with the calculated value of 65.5% according to the used complex concentration, which is carried out in air with heating rate of 10 °C min^{-1}.

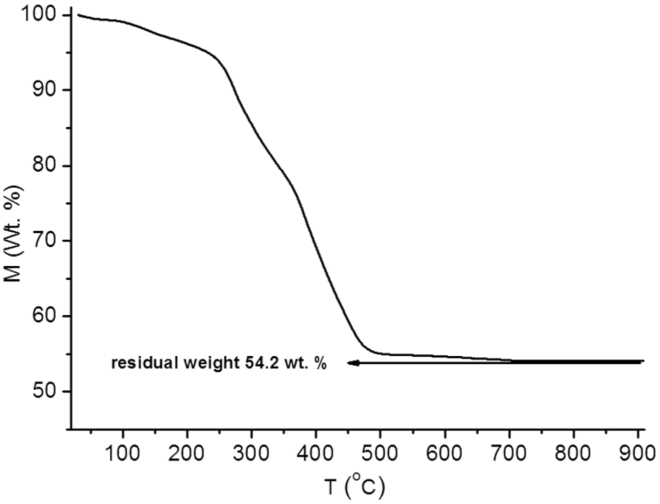

Figure S17. TGA curve of R-CSHC-86 with the residue of 54.2% at 900 °C, in agreement with the calculated value of 53.4% according to the used complex concentration, which is carried out in air with heating rate of 10 °C min^{-1}.

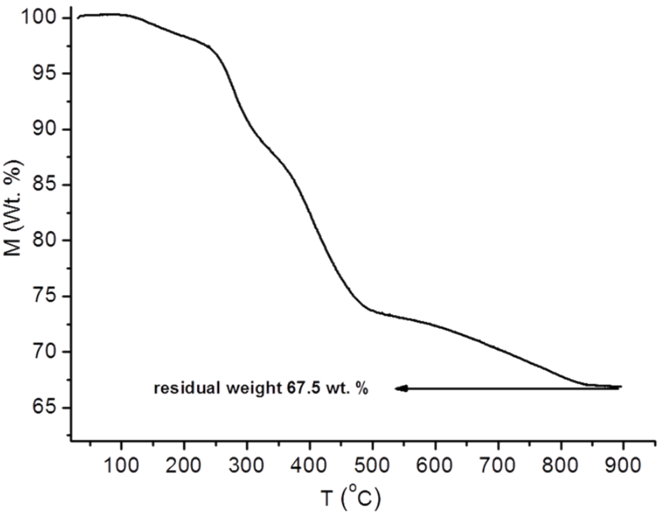

Figure S18. TGA curve of S-CSHC-58 with the residue of 67.5% at 900 °C, in agreement with the calculated value of 68.5% according to the used complex concentration, which is carried out in air with heating rate of 10 °C min^{-1}.

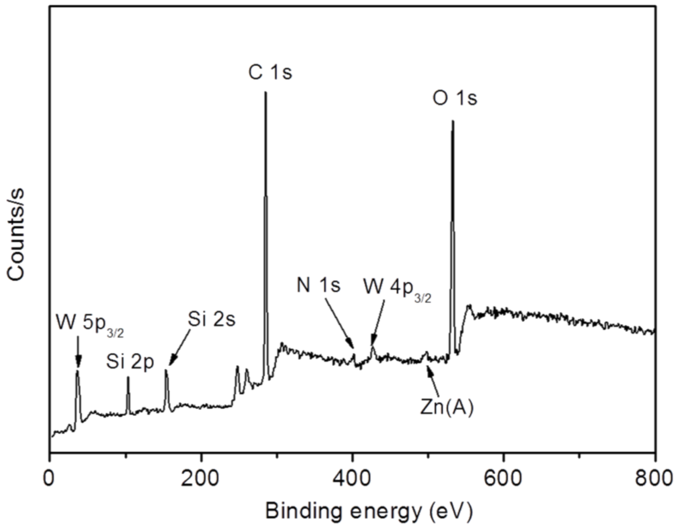

Figure S19. The XPS spectrum of R-CSHC-62, in which the evident existence of element Si, C, N, Zn, and W elements confirms the incorporation of R-CSEP complexes into the silica matrix.

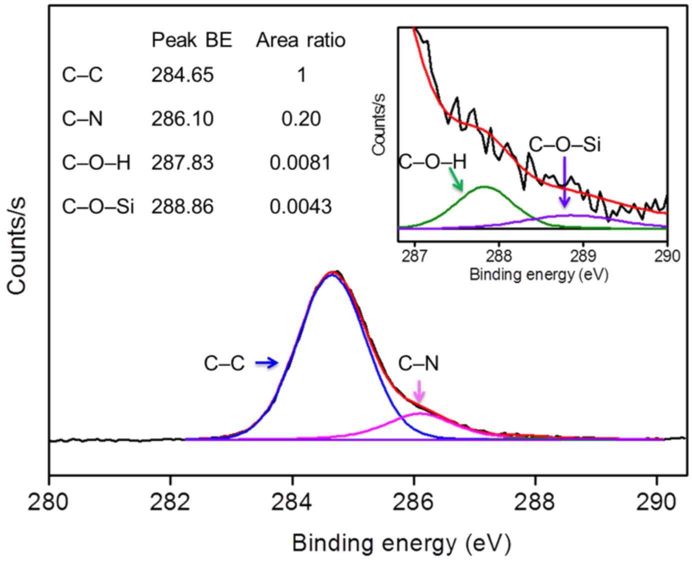

Figure S20. The XPS spectrum and simulation curves of C1s level of R-CSHC-62. Four types of C atoms are detected with peak binding energy at 284.65 (C–C), 286.10 (C–N), 287.83 (C–O–H), and 288.86 eV (C–O–Si).

Table S5. The analysis of surface element content of R-CSHC-62 and R-CSHC-86 from XPS data.

	Si [%]	C [%]	N [%]	W [%]	O [%]	Si/W	Si/N	Si/C
R-CSHC-62	12.35	59.01	1.67	1.44	25.53	7.40	8.58	0.21
R-CSHC-86	5.56	73.63	2.20	1.63	16.98	2.53	3.41	0.08

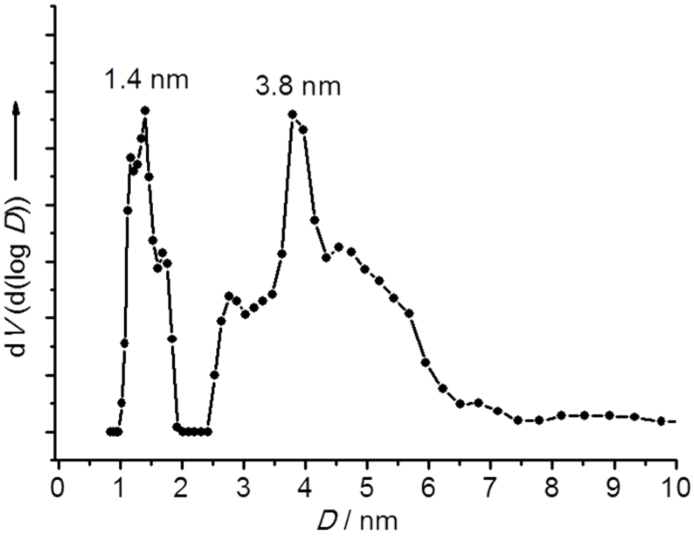

Figure S21. BJH pore size distribution plot of R-CSHC-0.

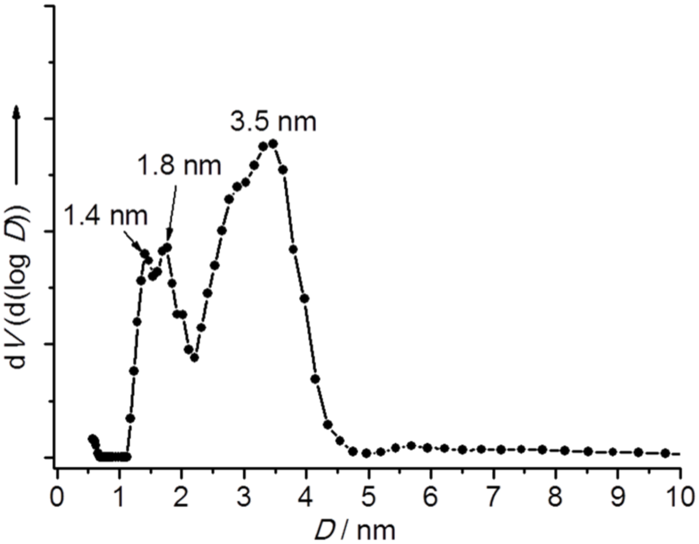

Figure S22. BJH pore size distribution plot of R-CSHC-30.

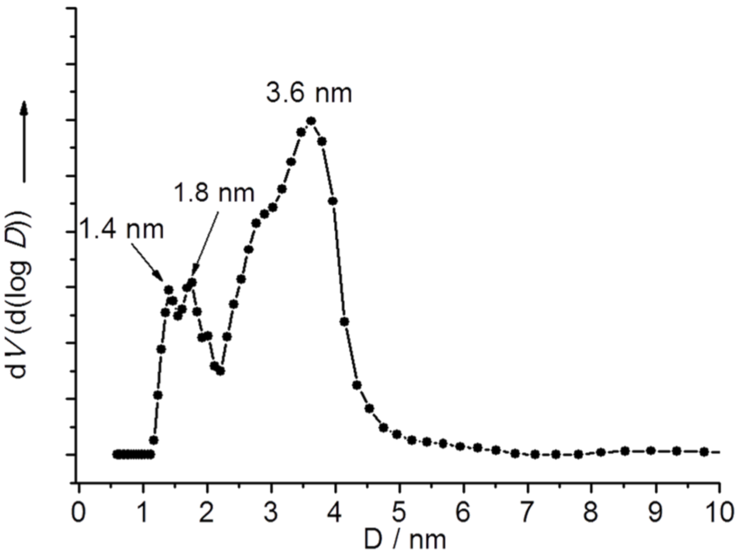

Figure S23. BJH pore size distribution plot of R-CSHC-46.

Table S6. The summary of pore parameters of R-CSHC-0, R-CSHC-30, R-CSHC-46, R-CSHC-62 and R-CSHC-86.[a]

Sample	surface area, S_{BET}, (m^2g^{-1})	pore volume, V,[b], (cm^3g^{-1})	BET pore, diameter,[c] (Å)
R-CSHC-0	410	0.34	38.2
R-CSHC-30	154	0.16	37.7
R-CSHC-46	77	0.08	33.7
R-CSHC-62	-	-	-
R-CSHC-86	-	-	-

[a] The pore parameters are measured from N_2 adsorption-desorption isotherms; [b] The pore volume is calculated by BJH method; [c] The average pore diameter is calculated from $4V/S_{\text{BET}}$ by BJH method.

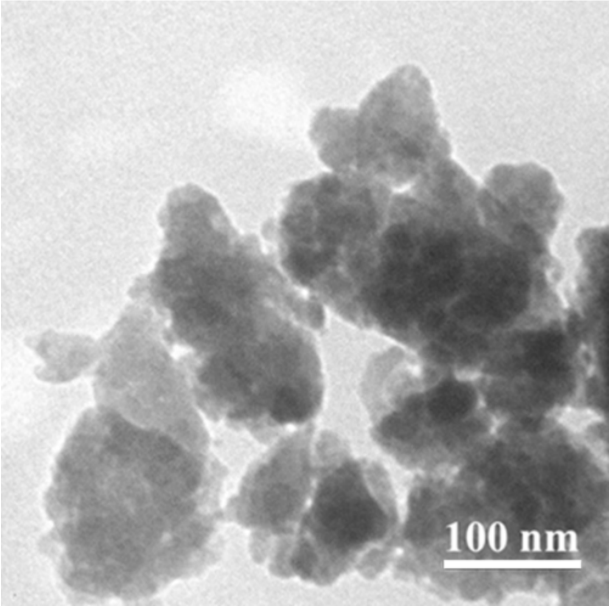

Figure S24. TEM image of freshly prepared R-CSHC-62 after being grinded to small particles with diameter about 100 nm.

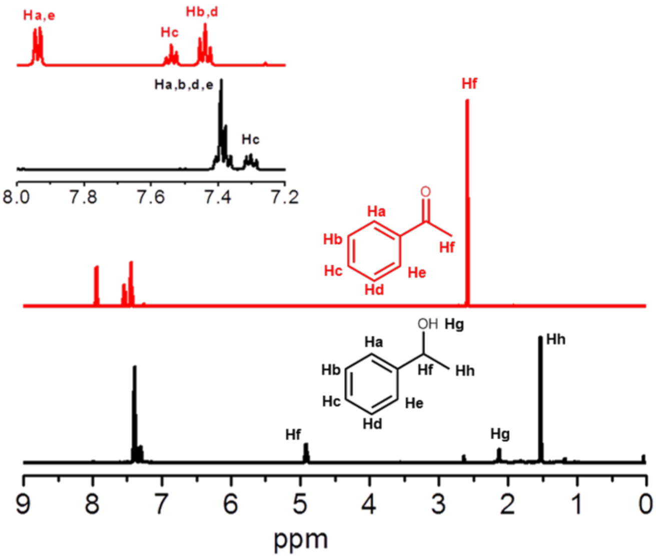

Figure S25. ^{1}H NMR spectra of racemic 1-phenylethanol (bottom, black line) and the product acetophenone (top, red line) in CD_3Cl.

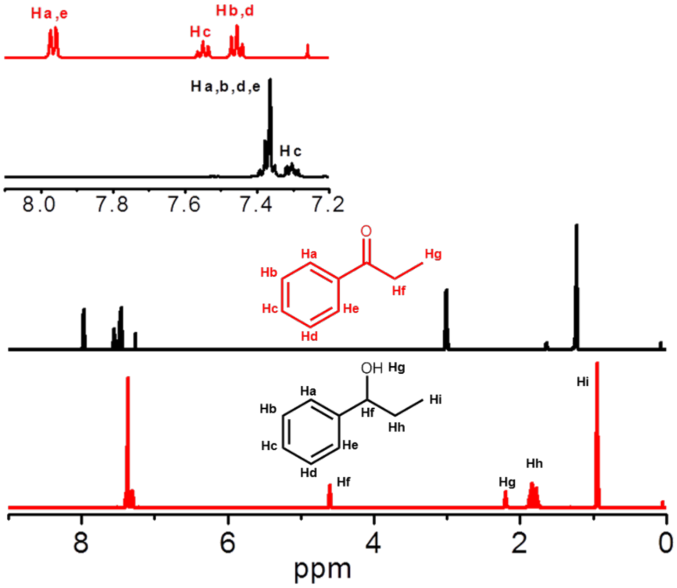

Figure S26. ^{1}H NMR spectra of racemic 1-phenylpropanol (bottom, black line) and the product propiophenone (top, red line) in CD_3Cl.

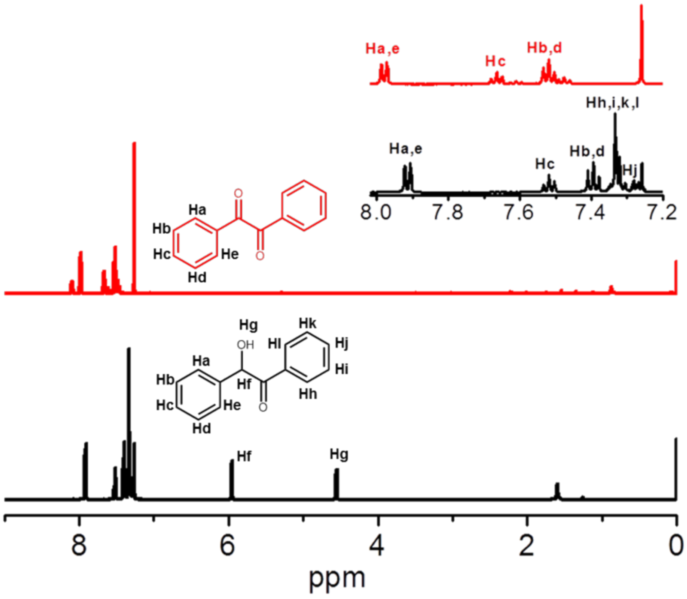

Figure S27. ^{1}H NMR spectra of racemic benzoin (bottom, black line) and the product benzil (top, red line) in CD_3Cl.

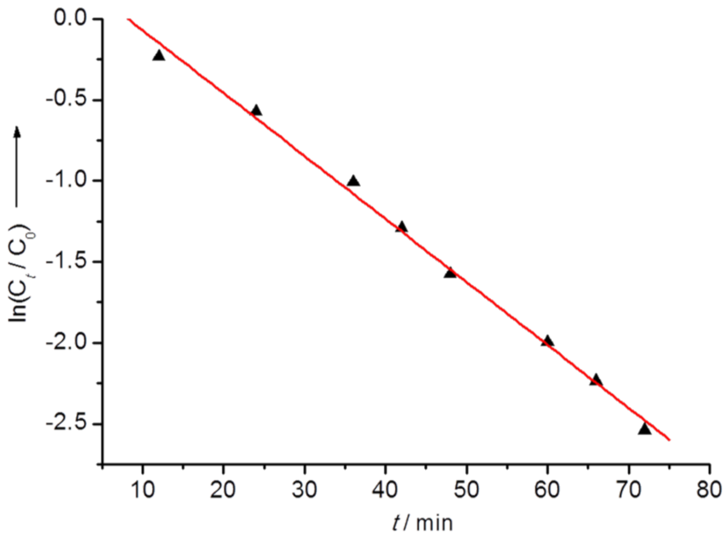

Figure S28. Plot of ln (C_t/C_0) versus reaction time *t* for the oxidation of benzoin in CH_3CN by using R-CSHC-86 as catalyst.

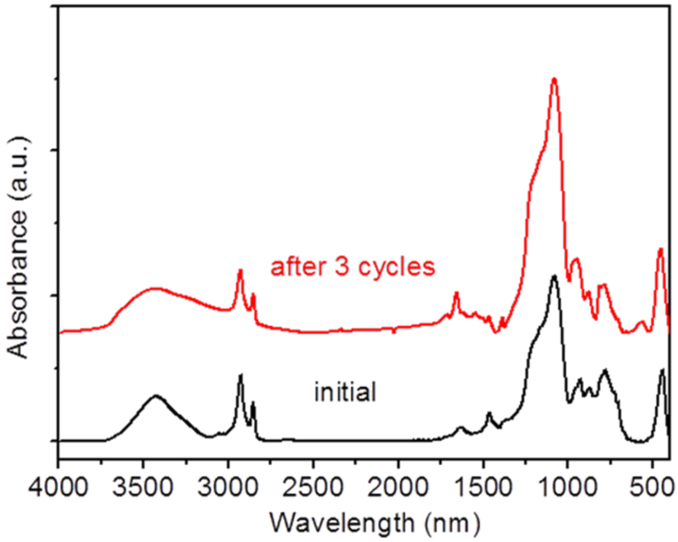

Figure S29. FT-IR spectra of freshly prepared R-CSHC-62 (bottom, black line) and the recycled one (top, red line) after 3-cycles in KBr pellets.

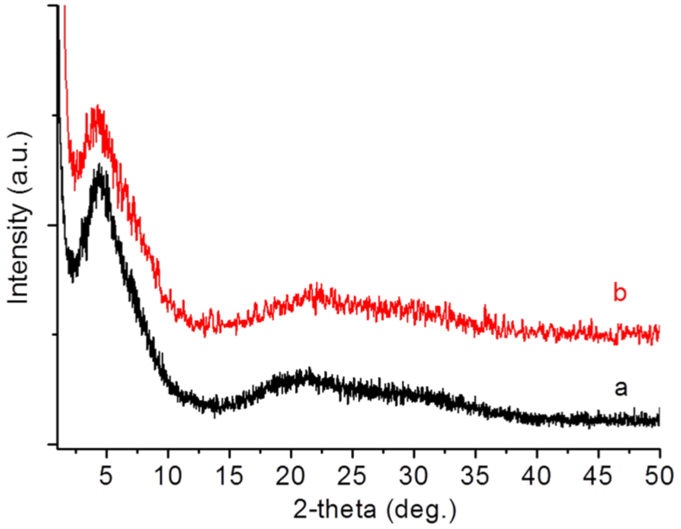

Figure S30. XRD spectra of (a) freshly prepared R-CSHC-62 and (b) the recycled R-CSHC-62.

Table S7. Recycling and reuse of the R-CSHC-62 in the oxidation of benzoin.[a]

Entry	*t* [h]	Conv. [%][b]	ee [%][c]
1	72	85.6	60.0
2	72	78.6	52.3
3	72	70.1	41.0

[a] All reactions are performed with benzoin (0.2 mM) and catalysts (1 µM) with R-CSHC-62 as catalysts in acetonitrile (1 mL); [b] The conversions are determined by HPLC based on the crude reaction mixture; [c] The ee values are determined by HPLC on a chiralcel OD-H column.

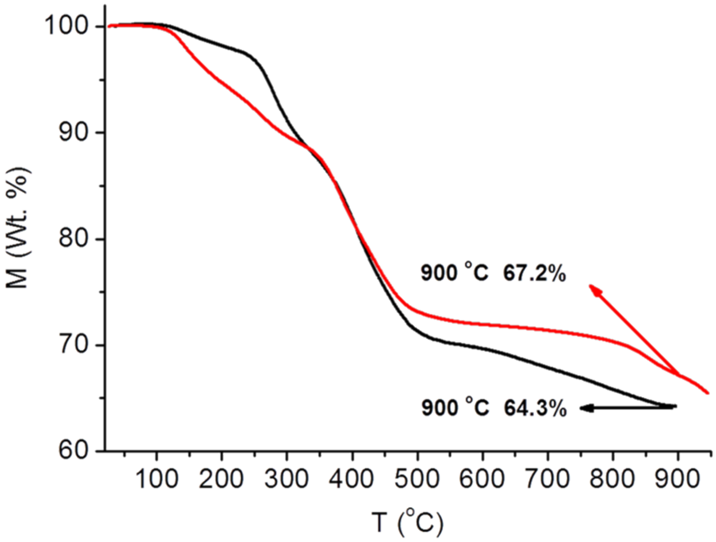

Figure S31. TGA curves of the original R-CSHC-62 (black line) and the recoverd R-CSHC-62 (red line), in which the experiments are carried out in air with a heating rate of 10 °C min^{-1}.

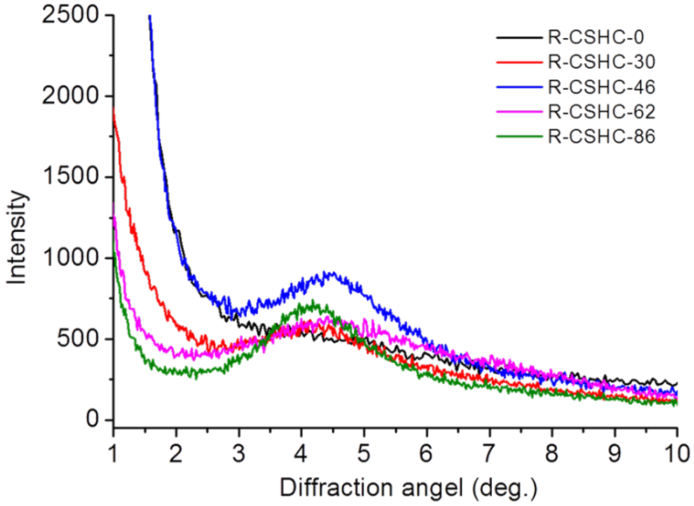

Figure S32. Small angle XRD patterns of R-CSHC-0, R-CSHC-30, R-CSHC-46, R-CSHC-62 and R-CSHC-86.

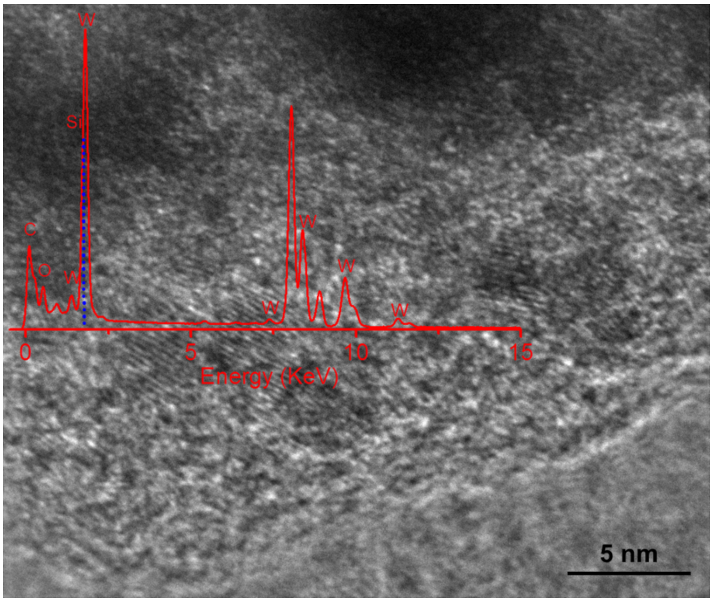

Figure S33. HR-TEM image of R-CSHC-86. The nanocrystalline domains could be clearly observed. The inset is corresponding EDX result, which suggests the composition of the nanocrystalline domains.

Table S8. The calculated surface density of chiral cations with different number of CSEP complexes in one nanocrystalline domain.

N_{cc}	Densest stacking state	Total free face number	Total chiral cations	Max. cation density	S_{coc} (nm^2)
1		6	1×12	2.0	1.14
2		10	2×12	2.4	1.37

3		14	3×12	2.6	1.48
4		16	4×12	3.0	1.71
5		20	5×12	3.0	1.71
6		22	6×12	3.3	1.88
7		24	7×12	3.5	2.00
8		24	8×12	4.0	2.28

N_{cc}: number of CSEP complexes in the nanocrystalline domain; S_{coc}: predicted surface area of chiral cations on the single face of a POM in aggregations.

Results of HPLC measurement:

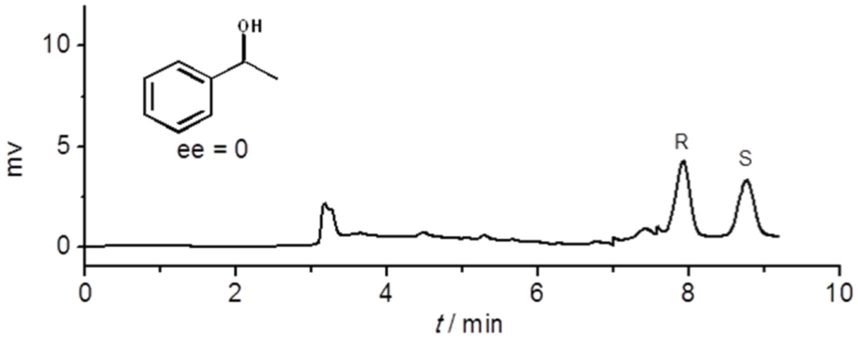

Figure S34. HPLC plot of racemic 1-phenylethanol under the conditions of chiralcel OD-H, flow rate: 1.0 mL min^{-1}, hexane/*i*PrOH = 95/5, and wavelength: 254 nm. Retention time: t_1 (*R*) = 7.93 min, t_2 (*S*) = 8.78 min.

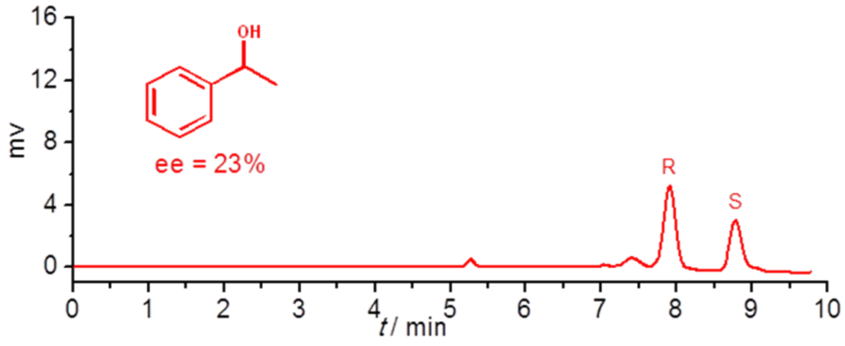

Figure S35. HPLC plot of 1-phenylethanol (*R*, 23% ee) under the conditions of chiralcel OD-H, flow rate: 1.0 mL min^{-1}, hexane/*i*PrOH = 95/5, and wavelength: 254 nm. Retention time: t_1 (*R*) = 7.90 min, t_2 (*S*) = 8.78 min.

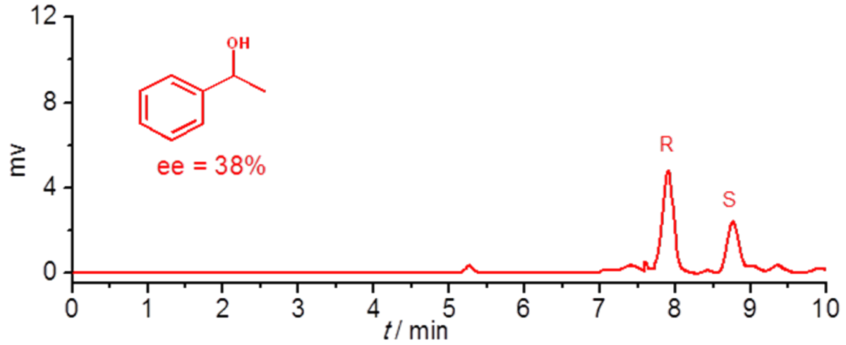

Figure S36. HPLC plot of 1-phenylethanol (*R*, 38% ee) under the conditions of chiralcel OD-H, flow rate: 1.0 mL min^{-1}, hexane/*i*PrOH = 95/5, and wavelength: 254 nm. Retention time: t_1 (*R*) = 7.90 min, t_2 (*S*) = 8.76 min.

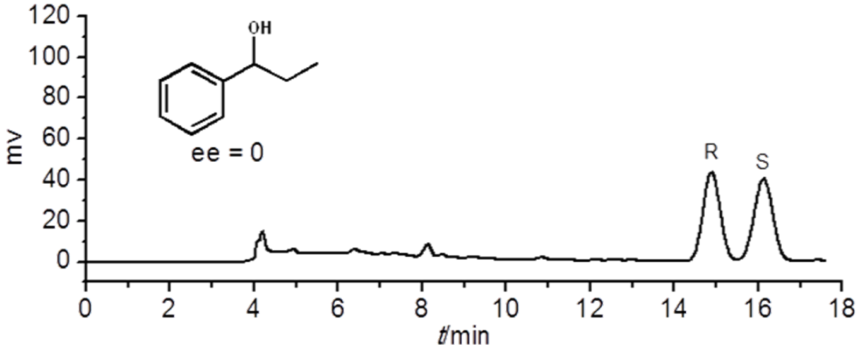

Figure S37. HPLC plot of racemic 1-phenylpropanol under the conditions of chiralcel OD-H, flow rate: 0.8 mL min^{-1}, hexane/*i*PrOH = 97.5/2.5, and wavelength: 254 nm. Retention time: t_1 (*R*) = 14.88 min, t_2 (*S*) = 16.14 min.

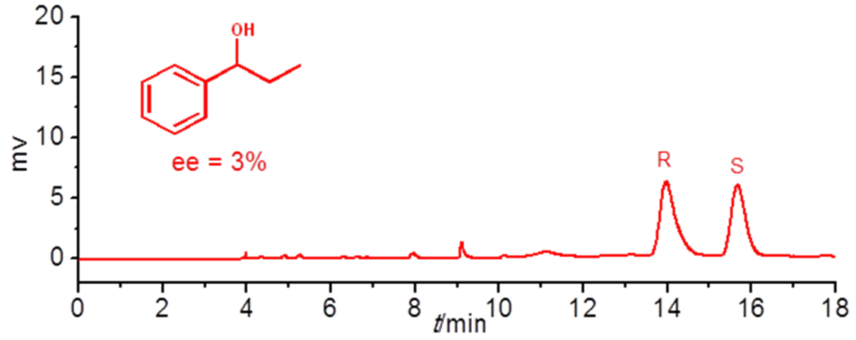

Figure S38. HPLC plot of racemic 1-phenylpropanol (*R*, 3% ee) under the conditions of chiralcel OD-H, flow rate: 0.8 mL min^{-1}, hexane/*i*PrOH = 97.5/2.5, and wavelength: 254 nm. Retention time: t_1 (*R*) = 13.98 min, t_2 (*S*) = 15.69 min.

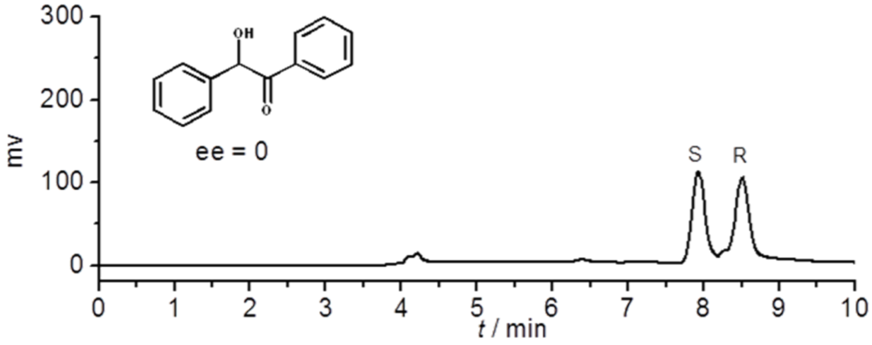

Figure S39. HPLC plot of racemic benzoin under the conditions of chiralcel OD-H, flow rate: 0.8 mL min^{-1}, hexane/*i*PrOH = 97.5/2.5, and wavelength: 254 nm. Retention time: t_1 (*S*) = 7.92 min, t_2 (*R*) = 8.52min.

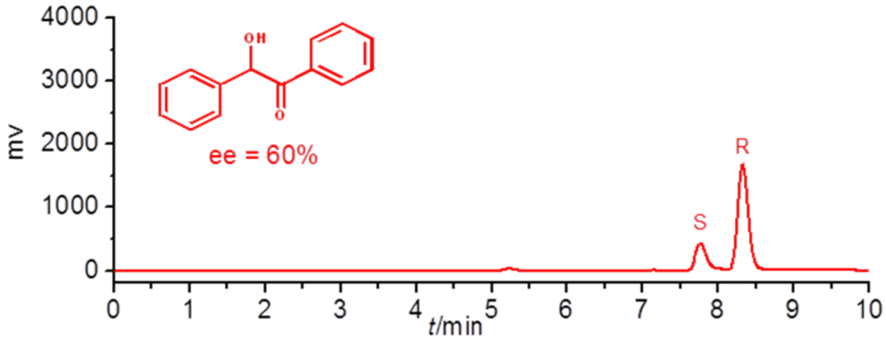

Figure S40. HPLC plot of benzoin (*R*, 60% ee) under the conditions of chiralcel OD-H, flow rate: 0.8 mL min^{-1}, hexane/*i*PrOH = 97.5/2.5, and wavelength: 254 nm. Retention time: t_1 (*S*) = 7.78 min, t_2 (*R*) = 8.33 min.

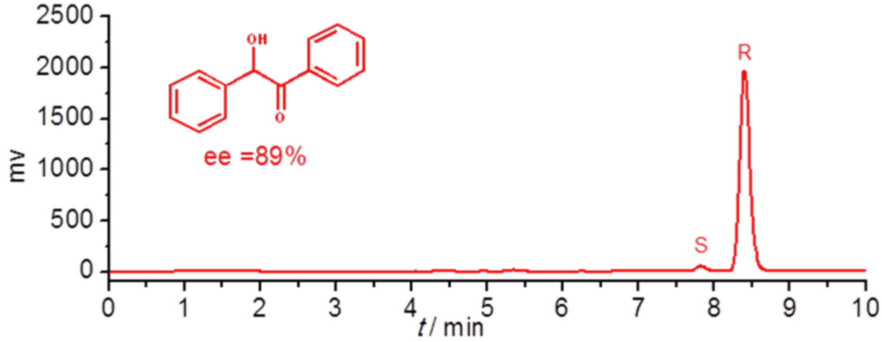

Figure S41. HPLC plot of benzoin (*R*, 89% ee) under the conditions of chiralcel OD-H, flow rate: 0.8 mL min^{-1}, hexane/*i*PrOH = 97.5/2.5, and wavelength: 254 nm. Retention time: t_1 (*S*) = 7.82 min, t_2 (*R*) = 8.40 min.

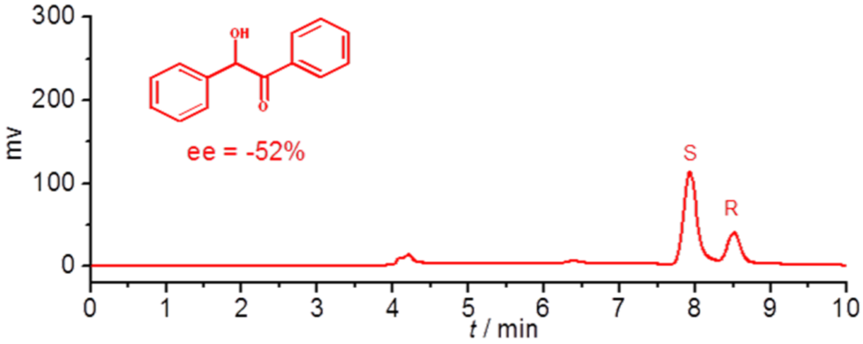

Figure S42. HPLC plot of racemic benzoin (*S*, 52% ee) under the conditions of chiralcel OD-H, flow rate: 0.8 mL min^{-1}, hexane/*i*PrOH = 97.5/2.5, and wavelength: 254 nm. Retention time: t_1 (*S*) = 7.93 min, t_2 (*R*) = 8.52min.